SUPPORTING INFORMATION

Simultaneous Electrochemical Monitoring of Metabolites Related to the Xanthine Oxidase Pathway Using a Grinded Carbon Electrode

Stanislav Hason[†], *Sona Stepankova*[‡] , *Alena Kourilova*[†], *Vladimir Vetterl*[†], *Jan Lata*[‡], *Miroslav Fojta*[†], *Frantisek Jelen*[†*]

[†] Institute of Biophysics, Academy of Sciences of the Czech Republic, v.v.i., Kralovopolska 135, CZ-61265 Brno, Czech Republic

[‡] Faculty Hospital Brno, Department of Internal Medicine and Gastroenterology, Jihlavska 20, CZ-625 00 Brno Bohunice, Czech Republic

*Corresponding Author: E-mail: jelen@ibp.cz, Fax: +420 541211293, Phone: +420 541517213

Voltammetric signals and mutual interference of UA, XAN, HYP, OXY and ALO

Table S-1 summarizes peak height of voltammetric peaks for individual purine derivatives (UA, XAN, OXY, HYP and ALO) or for four equimolar mixtures whose composition was chosen with respect to the model enzymatic reactions (OXY+ALO, UA+XAN+HYP, UA+XAN+OXY+HYP and UA+XAN+OXY+HYP+ALO, see Figures 2 and 4 in the article); concentration of all substances was always 650 nM. Presence of other components of the mixtures had insignificant effects on the peak potentials. On the other hand, one can see peak intensities were influenced by presence of other substances to certain extent. The most pronounced effect was observed in the case of XAN whose peak height was remarkably (by 48-68 %) increased in the presence of UA and other species. Enhancement of the peak intensity was also observed for UA but the relative change was smaller in this case (10-13 %). Such behavior may be connected with interaction between various analytes and/or products of their oxidation at the electrode surface, possibly facilitating their accumulation or electrooxidation. The phenomenon will be further studied in details and results will be published elsewhere. Peaks of HYP and ALO were suppressed in mixtures containing both species, compared to pure individuals, which may be caused partly by proximity of both, mutually overlapping signals.

Table S-1

Solution content	Current densities of oxidation peaks of each of monitored component				
	UA[a] (+0.432 V)[b]	XAN[a] (+0.754 V)[b]	OXY[a] (+0.925 V)[b]	HYP[a] (+1.076 V)[b]	ALO[a] (+1.157 V)[b]
			μA cm^{-2}		
UA	23.38 ± 0.72				
XAN		3.80 ± 0.31			
OXY			10.84 ± 0.54		
HYP				4.48 ± 0.12	
ALO					5.66 ± 0.20
OXY+ALO			9.80± 0.48		4.50 ± 0.25
UA+XAN+HYP	26.50 ± 1.28	6.42 ± 0.39		3.94 ± 0.40	
UA+XAN+OXY+HYP	25.70 ± 0.97	5.63 ± 0.21	9.20 ± 0.36	3.42 ± 0.16	
UA+XAN+OXY+HYP+ALO	26.30 ± 1.00	5.92 ± 0.72	11.18 ± 0.38	1.44 ± 0.07	2.55 ± 0.02

[a] concentration 650 nM
[b] oxidation peak potential of each of monitored component

Figure S-1 shows calibration curves for UA and equimolar mixtures of XAN+OXY+HYP, UA+XAN+OXY+ HYP, and OXY+ALO. Except for HYP that exhibited remarkably sub-

linear dependence of its peak height on concentration in both cases, all substances showed linear calibration plots to 2 μM (at the given conditions, the lowest detectable concentration for UA and other substances was 25 nM). Slopes of the relevant calibration plots, obtained for individual compounds (Figure S-1A, B, C and D), were only slightly influenced by the mixture composition (differences were not higher that units of %).

Figure S-1

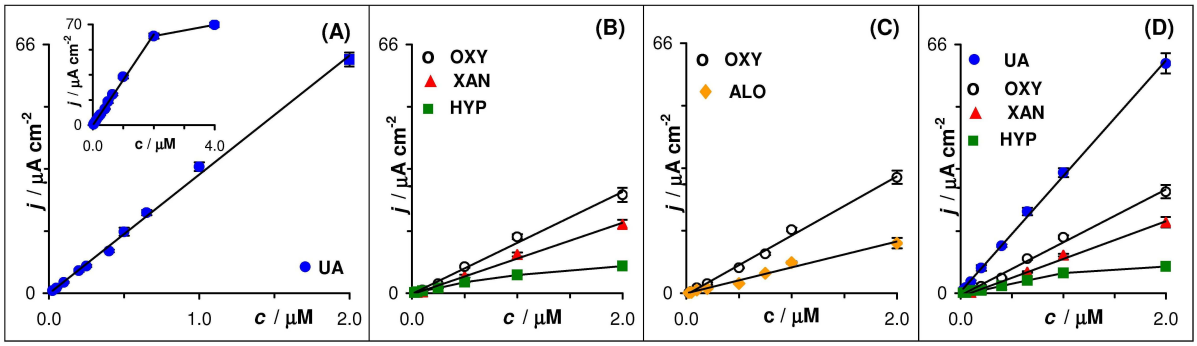

Figure S-1. *Concentration dependences of the current densities of the oxidation signals of (●) UA (A); for equimolar mixtures of (▲) XAN, (o) OXY and (■) HYP (B); for equimolar mixtures of (o) OXY and (♦) ALO (C); and for equimolar mixtures of (●) UA, (▲) XAN, (o) OXY, and (■) HYP (D). The measurements were performed in 0.1 M acetate buffer at mechanically grinded (with 15 μm SiC particles) edge plane-oriented pyrolytic graphite electrode (g-PGEe) in 0.1 M acetate buffer, pH 4.8, at room temperature. Accumulation conditions, E_A = +0.2 V; t_A = 2 min; rate of stirring ω = 3000 min^{-1}.*

Grinded carbon electrodes

The advantages of grinded carbon electrodes in determination of uric acid, other purine derivatives as well as some other bioactive substances have been reported previously [1]. Here we show voltammetric responses of a mixture of UA, XAN, HYP, ALO and OXY at two grinded electrodes in comparison with other carbon electrode types (polished and/or electrochemically activated) (Figure S-2). One can see that only the mechanically grinded edge plane-oriented pyrolytic graphite electrode provides: (i) well-separated oxidation signals for XAN, OXY, HYP and ALO in the presence of an excess of UA, and (ii) no background current perturbations interfering with analytical signals within the studied potential range.

Figure S-2

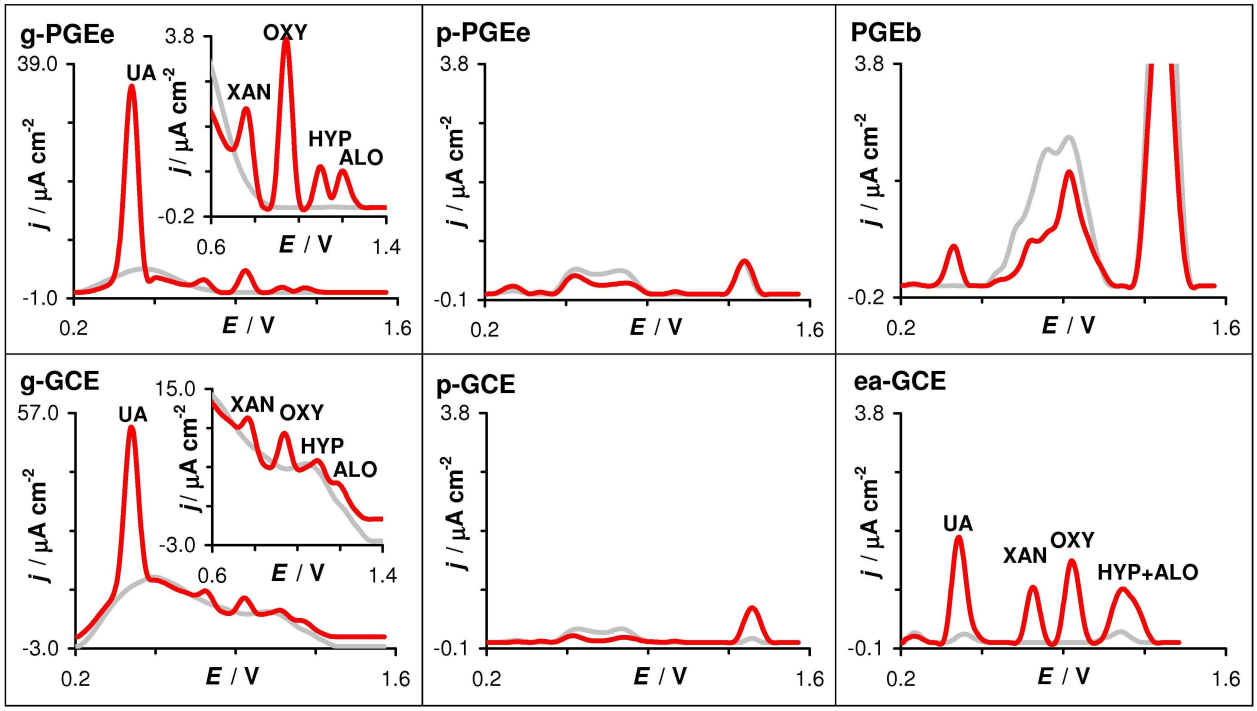

Figure S-2. *Anodic stripping DPVs measured for mixtures of UA (1 µM), XAN, OXY, HYP, and ALO (each of 200 nM) at different carbon-based electrodes (red lines). Gray lines represent the blank responses (0.1 M acetate buffer alone). Abbreviation of the electrodes are given on the left top corner: g-PGEe mechanically grinded (with 15 µm SiC particles) edge plane-oriented pyrolytic graphite electrode; g-GCE mechanically grinded (with 15 µm SiC particles) glassy carbon electrode; p-PGEe or p-GCE fine polished (with 1 µm abrasion particles) PGEe or GCE; ea-GCE electrochemically activated fine polished GCE; PGEb freshly cleaved basal plane-orientated pyrolytic graphite electrode. Accumulation conditions:* E_A *= +0.2 V;* t_A *= 2 min; rate of stirring* $\omega = 3000\ min^{-1}$.

Effect of ascorbic acid on detection of UA, XAN, HYP, ALO and OXY at grinded electrode.

Previously [1] we have shown that large (three orders of magnitude) excesses of ascorbic acid (AA) only negligibly affected voltammetric signals of UA at the grinded electrodes, which was ascribed to rather weak (compared to UA) adsorption of AA at the electrode surface. Here we tested influence of AA on the DPV responses of UA, XAN, HYP, OXY and ALO.

Results summarized in Figure S-3 and Table S-2 confirm that voltammetric signal of AA is sufficiently separated from that of UA (about 380 mV at our experimental conditions) and only small changes in peak heights are observed at high excess of AA. Differences are within 4-5 %, i.e. within the same range as the experimental error [1]. With the exception of ALO (whose peak was influenced more significantly), changes in the peak heights of other substances did not exceed 10% or 20% for 1,000-fold and 5,000-fold excess of AA, respectively (this is particularly important for UA, XAN and OXY which are the excreted metabolites monitored in urine where presence of potentially interfering AA can be expected).

Figure S-3

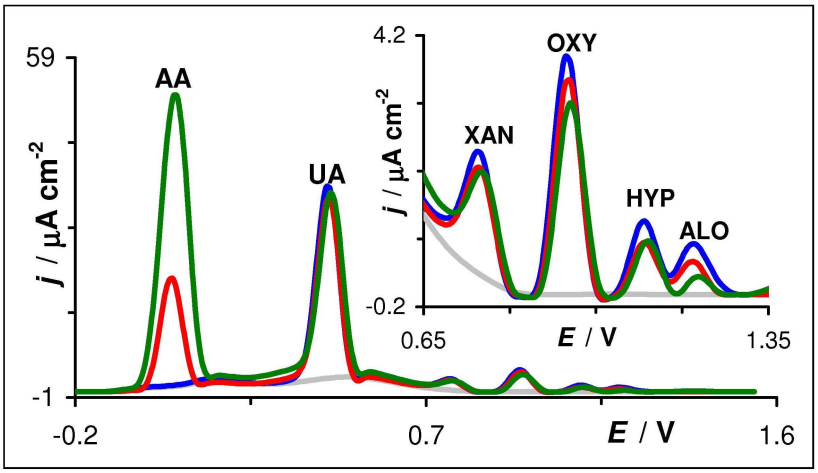

Figure S-3. *Baseline-corrected differential pulse voltammogram responses for mixtures of 1 µM UA + 200 nM XAN + 200 nM OXY + 200 nM HYP + 200 nM ALO (blue); 200 µM AA + 1 µM UA + 200 nM XAN + 200 nM OXY + 200 nM HYP + 200 nM ALO (red); and 1000 µM AA + 1 µM UA + 200 nM XAN + 200 nM OXY + 200 nM HYP + 200 nM ALO (green) in 0.1 M acetate buffer (pH ~4.8) measured at g-PGEe. Gray lines represent the blank responses. Accumulation conditions:* E_A *= -0.2 V;* t_A *= 2 min; rate of stirring* $\omega = 3000\ min^{-1}$.

Table S-2

AA increment to the purine derivatives solution mixture μM	Current densities of oxidation peaks for monitored components					
	AA (+0.052 V)[c]	UA[a] (+0.432 V)[c]	XAN[b] (+0.754 V)[c]	OXY[b] (+0.925 V)[c]	HYP[b] (+1.076 V)[c]	ALO[b] (+1.157 V)[c]
	μA cm^{-2}					
0		34.4 ± 1.0	1.74 ± 0.11	3.96 ± 0.38	1.04 ± 0.10	0.65 ± 0.04
200	19.3 ± 0.3	32.4 ± 1.6	1.48 ± 0.10	3.52 ± 0.44	0.78 ± 0.01	0.42 ± 0.02
1000	51.0 ± 1.4	32.2 ± 0.9	1.33 ± 0.13	3.16 ± 0.10	0.90 ± 0.03	0.30 ± 0.03

[a] concentration 1 μM
[b] concentration 200 nM
[c] oxidation peak potential of each of monitored component

Electroactivity of xanthine oxidase

In experiments focused on monitoring enzymatic conversion of purine derivatives (Figure S-4A,B) we observed a signal at potential about +0.75 V (i.e., close to the oxidation peak of XAN) regardless of addition of XAN or HYP (being converted primarily to XAN). In absence of HYP and/or XAN the height of this peak did not change with time, and analogous peak was detected also after prolonged incubation of the reaction mixture when all HYP and XAN were expected to be converted into UA. We found that this voltammetric signal is produced by XO itself. Figure S-4A shows that intensity of the signal increased with concentration of the XO. We tentatively attributed the peak to oxidation of tyrosine residues [2-4] in the enzyme; such assumption is supported by analogous behavior of another Tyr-containing protein, ribonuclease A (Fig. S-4B), and by its irreversibility (as documented by cyclic voltammetry, see inset in Fig S-4A). For higher XO concentration, additional two more positive (+ 1.0 V and +1.15 V) signals appeared which may be related to other electroactive components of the XO holoenzyme - molybdopterin, Fe_2S_2 iron sulfur centers and/or FAD (40 kDa) [5].

Figure S-4

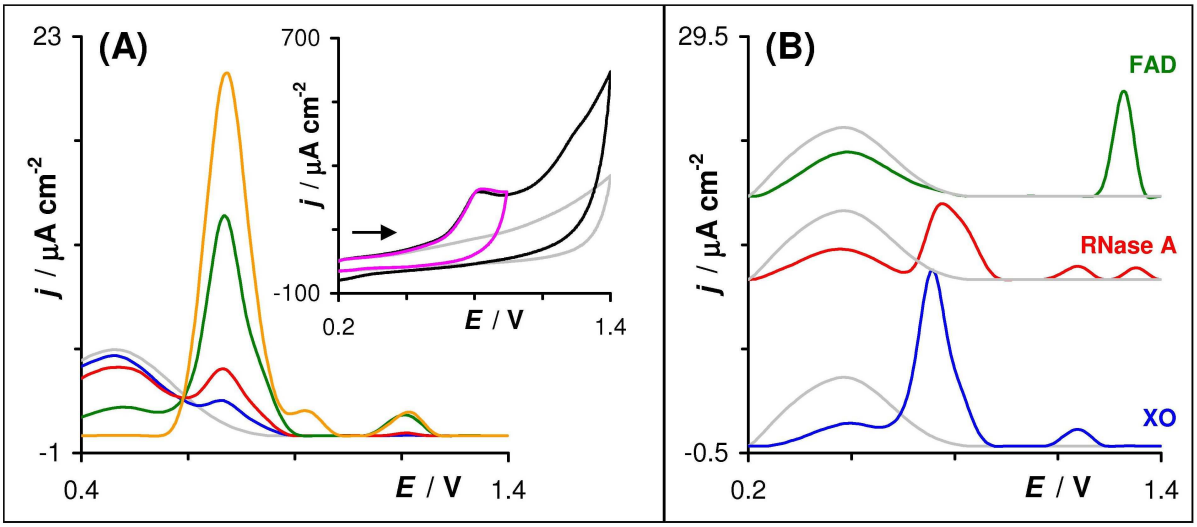

Figure S-4. *(**A**) The baseline-corrected DPVs of XO at different concentrations measured at g-PGEe: (blue) 0.15 µU mL^{-1} (2.78 nM); (red) 2.25 µU mL^{-1} (41.7 nM); (green) 22.5 µU mL^{-1} (0.417 µM); and (yellow) 225 µU mL^{-1} (4.17 µM). Gray line represents the blank response (0.1 M acetate buffer, pH 4.8). Inset shows cyclic voltammograms for g-PGEe measured in blank 0.1 M acetate buffer (gray curve) and in 0.1 M acetate buffer containing 225 µU mL^{-1} (4.17 µM) XO (black and pink curve). Initial potential +0.2 V; switching potential +1.4 V (gray and black curves) or +0.942 V (pink curve), respectively, scan rate 100 mV s^{-1}. (**B**) The baseline-corrected DPVs for 4.17 µM XO (blue); 1 µM RNase A (red); and 1 µM FAD (green) in 0.1 M acetate buffer measured at g-PGEe. Grey lines represent the blank responses (0.1 M acetate buffer). Curves for RNase A and FAD are shifted along the current density axis by +12 and +18, respectively, for better resolution. Other conditions were the same as in the Figure S-1.*

Determination of UA and interferences of other substances in diluted urine

To test the accuracy of measurements in diluted urine samples we compared electrochemical and enzymatic (spectrophotometrical) method for buffer solution of synthetic UA, "natural" sample U3 diluted 1,000-, 2,000- or 4,000-fold (containing, when non-diluted, 1 mM UA, as determined by the enzymatic method), and the diluted urine with standard additions of synthetic UA. Results summarized in Figure S-5A (for more details see the legend) shows an excellent proportionality between the peak height and UA concentration for all urine dilutions

and UA concentrations. Further, we tested the effect of added XAN and OXY concentration on the peak height of UA in the 1000-fold diluted urine sample U3. Thus, equimolar mixture of XAN and OXY at concentrations between 50 nM to 2 μM (of each) was added to 1 μM UA solution and changes of UA peak height were followed. Figure S-5B shows no significant effect on UA peak height at XAN and OXY concentrations up to 0.25 μM. At higher concentration of XAN and OXY, the UA peak slightly increased in agreement with results obtained for mixtures of synthetic substances (see above)

Figure S-5

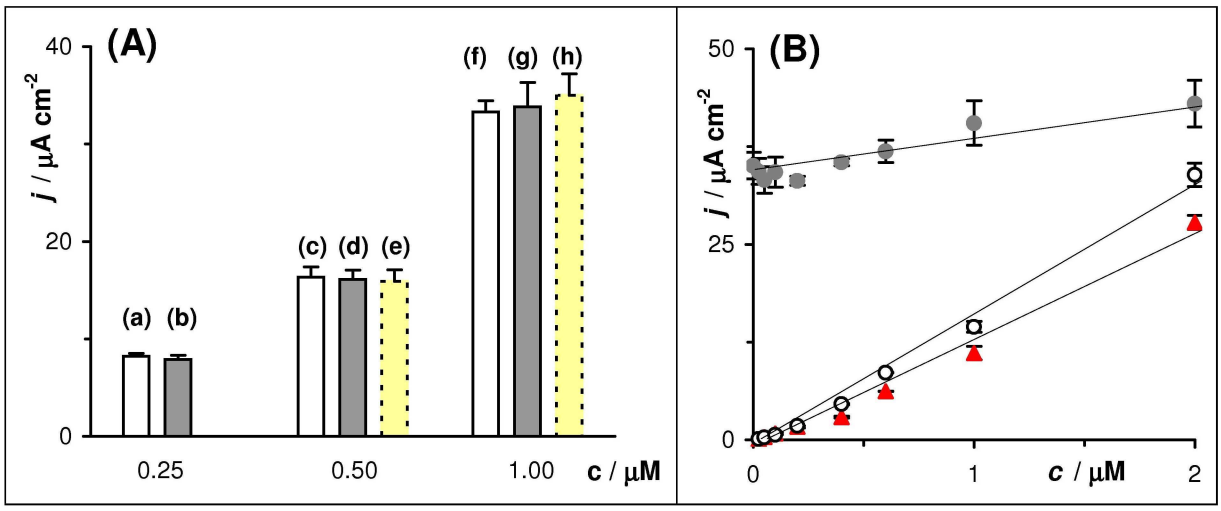

Figure S-5. *(**A**) Current densities of the UA oxidation signal measured for: 0.25 μM synthetic UA solution (a); 4,000-fold diluted urine U3 (b); 0.5 μM synthetic UA solution (c); 2,000-fold diluted urine U3 (d); sample b with addition of 0.25 μM synthetic UA (e); 1.0 μM synthetic UA solution (f); 1,000-fold diluted urine U3 (g); sample d with addition of 0.5 μM synthetic UA (h). UA concentration in non-diluted urine U3, determined by standard enzymatic method, was 1.0 mM (see Table 1 in the article). (**B**) Effect of XAN and OXY concentration on UA oxidation signal in the 1,000-times diluted U3 sample. XAN and OXY were added in equimolar concentrations as indicated in the graph; current density of UA oxidation signal (●); the same for signals of the added XAN and OXY, (▲ and ○, respectively). Other conditions were the same as in the Figure S-1.*

References

(1) Hason, S.; Vetterl, V.; Jelen, F.; Fojta, M. *Electrochim. Acta* **2009**, *54*, 1864-1873.

(2) Armstrong, F. A. In *Encyclopedia of Electrochemistry. Bioelectrochemistry*; Wilson, G. S., Ed.; Wiley-VCH: Weinheim, 2002; Vol. 9, pp 11-29.

(3) Ferapontova, E.; Shleev, S.; Ruzgas, T.; Stoica, L.; Christenson, A.; Tkac, J.; Yaropolov, A. I.; Gorton, L. In *Perspectives in Bioanalysysis. Vol. 1 Electrochemistry of nucleic acids and proteins. Towards electrochemical sensors for genomics and proteomics*; Palecek, E., Scheller, F., Wang, J., Eds.; Elsevier: New York, 2005; Vol. 1, pp 517-598.

(4) Palecek, E. In *Perspectives in Bioanalysysis. Vol. 1 Electrochemistry of nucleic acids and proteins. Towards electrochemical sensors for genomics and proteomics*; Palecek, E., Scheller, F., Wang, J., Eds.; Elsevier: New York, 2005; Vol. 1, pp 690-750.

(5) Borges, F.; Fernandes, E.; Roleira, F. *Curr. Medicin. Chem.* **2002**, *9*, 195-217.